NASA TECHNICAL NOTE

NASA TN D-3455

c. 1

NASA TN D-3455

WIND-TUNNEL INVESTIGATION OF SONIC-BOOM CHARACTERISTICS OF A DELTA-WING-BODY COMBINATION AT MACH NUMBERS OF 1.41 AND 2.01

by Odell A. Morris

Langley Research Center
Langley Station, Hampton, Va.

NATIONAL AERONAUTICS AND SPACE ADMINISTRATION • WASHINGTON, D. C. • JUNE 1966

WIND-TUNNEL INVESTIGATION OF SONIC-BOOM CHARACTERISTICS OF A DELTA-WING-BODY COMBINATION AT MACH NUMBERS OF 1.41 AND 2.01

By Odell A. Morris

Langley Research Center
Langley Station, Hampton, Va.

NATIONAL AERONAUTICS AND SPACE ADMINISTRATION

For sale by the Clearinghouse for Federal Scientific and Technical Information
Springfield, Virginia 22151 – Price $1.00

WIND-TUNNEL INVESTIGATION OF SONIC-BOOM CHARACTERISTICS OF A DELTA-WING-BODY COMBINATION AT MACH NUMBERS OF 1.41 AND 2.01

By Odell A. Morris
Langley Research Center

SUMMARY

An investigation has been conducted in the Langley 4- by 4-foot supersonic pressure tunnel at Mach numbers of 1.41 and 2.01 to determine the sonic-boom characteristics of a delta-wing-body model. Pressure signatures were measured for the model with the wedge-shaped body both above and below the wing.

Results of the tests showed that the measured adjusted maximum pressure-rise values over the positive lift range tested were larger for the low-wing model than for the high-wing model. Comparison of the experimental and theoretical results showed good agreement which indicates that the large lift interference effects produced by the wedge-shaped body can be evaluated theoretically to obtain reasonable estimates of the sonic-boom overpressures.

INTRODUCTION

Design studies of several versions of the commercial supersonic transport have indicated that the sonic-boom problem is a major one for configurations of this type. As a result, a number of research studies have been made to provide theoretical and experimental data on sonic-boom overpressures and to develop methods of reducing these overpressures. (See refs. 1 to 3.) In general, these studies have indicated that the sonic-boom overpressures could be predicted reasonably well with the available theoretical methods and have shown possible ways to minimize sonic-boom overpressures for transport configurations.

As part of the continuing program on sonic-boom research, an investigation of the sonic-boom characteristics of an unsymmetrical model has been made. The purpose of the investigation was to determine if sonic-boom pressures may be reduced by employing a low-wing configuration whereby the wing acts as a shield to prevent the pressures generated by the body from being transmitted to the ground. In addition, calculations were made to determine if the theory can adequately predict the sonic-boom pressures for an unsymmetrical model configuration on which large wing-body interference effects occur.

The experimental investigation was undertaken in the Langley 4- by 4-foot supersonic pressure tunnel to measure the sonic-boom characteristics of a delta-wing-body combination. The model incorporated a wedge-shaped body that was designed to produce large interference effects on the wing. The body was positioned rearward on the wing planform so that the interference pressures generated by the body would be confined to one surface of the wing. The model was tested with the wedge-shaped body both above and below the wing at Mach numbers of 1.41 and 2.01. The pressure signatures of the models were measured for several angles of attack and various vertical distances from the models. The normal force of the models was measured by use of a miniature one-component internal strain-gage balance. Results of the tests have been compared with theory and are presented herein.

SYMBOLS

Measurements were taken in the U.S. Customary System of Units. Equivalent values are indicated herein parenthetically in the International System of Units (SI). Details concerning the use of SI, together with physical constants and conversion factors, are given in reference 4.

A	cross-sectional area of model
$A(t)$	nondimensional cross-sectional area of model, A/l^2
B	equivalent cross-sectional area of model due to lift
$B(t)$	nondimensional equivalent cross-sectional area of model due to lift, B/l^2
C_L	lift coefficient
h	airplane flight altitude or perpendicular distance from model to measuring probe
K_r	reflection factor, 1.0
l	reference length of model
M	Mach number

p free-stream static reference pressure

Δp incremental pressure due to flow field of model

$\left(\frac{\Delta p}{p}\right)_{max}$ maximum pressure ratio at bow shock

S reference wing area

Δx distance from point on pressure signature to point where pressure signature curve crosses zero-pressure reference axis

x' distance from nose measured along model axis

α angle of attack

$\beta = \sqrt{M^2 - 1}$

MODEL AND TESTS

A drawing of the test model is shown in figure 1. The wing had flat-wing sections with a sharp leading edge which was swept back 52.5°. The wing was constructed from a high-quality single-edge razor blade that was 0.009 inch (0.023 cm) thick. The fuselage was a wedge-shaped body with rectangular cross sections and had a leading-edge wedge angle of 25°. The fuselage nose was located rearward of the wing apex so that the shock associated with the body would be largely shielded behind the leading edge of the wing and thus would restrict the interference pressures generated by the wedge-shaped body to one side of the wing surface. At the lower Mach number of 1.41, the shock from the body would probably extend slightly forward of the wing leading edge in the region of the wing tip.

The tests were conducted in the Langley 4- by 4-foot supersonic pressure tunnel at Mach numbers of 1.41 and 2.01 with a stagnation pressure of 10 psi (69kN/m^2) and a stagnation temperature of 100° F (311° K). A sketch of the test apparatus is shown in figure 2. Both the model and the measuring probe were mounted on a support system which provided for remotely controlled adjustments of the probe and model positions. The angle of attack of the model was set manually after each run through the use of a sting mounting strut with provisions for the various angle-of-attack settings desired. The fuselage of the model contained a one-component internal strain-gage balance which measured the normal-force component for the angle-of-attack range investigated. The small balance measured only 0.625 inch (1.59 cm) in length and had a design load of 0.6 pound (2.7N).

The measuring probes were very slender cones (1° cone angle) with four 0.013-inch-diameter (0.033 cm) static pressure orifices leading to a common chamber. Orifices were spaced 90° apart around the probe and were arranged to lie in a Mach 1.41 cone originating at the model. For the Mach number range tested, changes in the Mach cone angle with respect to the orifice spacing have no significant effect on the measured pressures. The pressures were measured by using a differential pressure gage with a 0.10 psi ($0.69 kN/m^2$) design load. Further details on the wind-tunnel sonic-boom test technique are given in reference 1.

RESULTS AND DISCUSSION

The results of references 2 and 3 have shown that for some high-fineness-ratio models or equivalent body shapes, far-field conditions would be reached only at considerable distances from the model which would be well beyond the space limits of the tunnel. Under these nonasymptotic conditions, the near-field theory would be used to calculate the sonic-boom overpressures as described in reference 2. However, because of the unusually low fineness ratio of the present test model, the theoretical far-field conditions would develop rapidly at only a short distance from the model and, therefore, the far-field theory was used for comparison with the measured overpressures.

Figure 3 shows the distribution of the nondimensionalized effective cross-sectional area and the nondimensional equivalent cross-sectional area due to lift for the model that were used in calculating the theoretical far-field sonic-boom overpressures; these distributions were obtained from a machine computing program as outlined in reference 1. The effective cross-sectional-area curve includes the equivalent cross-sectional area due to the interference lift produced by the wedge at $\alpha = 0^{\circ}$ and also includes an estimate of the area distribution under a laminar boundary layer.

Measurement of the pressure signatures for the model at the various test conditions are shown in figure 4. Pressures and distances are plotted in parametric form in accordance with theoretical considerations. According to theory, the far-field pressure signatures for a given model and lifting condition when plotted in this form should be identical for the various distances and should assume a characteristic N-shape. For the pressure signatures measured at the low angles of attack, the data indicated that complete far-field conditions have not been obtained. (For example, see fig. 4(a).) In order to compensate for the lack of attainment of far-field conditions as well as to account for the probe boundary layer and for the effects of vibration of the test equipment, the maximum pressure-rise ratio at the bow shock was adjusted by using the method described in reference 1 (Appendix B). The adjusted values are shown on each of the measured signatures in figure 4 as a dashed line.

The adjusted tunnel sonic-boom data are compared with the far-field theoretical values in figure 5. The pressure-rise parameter has been plotted against the lift parameter for the model in upright and inverted positions with data for each of the three vertical distances shown. Reasonably good agreement is shown between the theoretical and experimental values. To show a direct comparison of the effects of the model in the upright and inverted positions, the data are replotted and shown in figure 6 with the data for the three vertical distances plotted as average values. For both Mach numbers, the upright model (body on top of the wing) has higher values of the pressure parameter for the higher positive values of the lift parameter. However, for the negative values of the lift parameter, the trend is reversed and, at $M = 2.01$, fairly large differences between the upright and inverted models were measured.

The average values of the adjusted experimental pressure parameters are shown in figure 7 plotted against both angle of attack and lift coefficient for the upright and inverted models. This figure illustrates the magnitude of the interference effects between the body and wing due to body position. At both Mach numbers, it may be noted that with the body below the wing, the pressure parameter values were larger throughout the angle-of-attack range because of the positive pressures and resulting higher lift values produced by the wedge-shaped body. With the body above the wing, similar positive interference pressures due to the body occur that decrease the lift. Thus, to obtain a lift coefficient of about the same magnitude, the low-wing model requires an angle of attack about $1\frac{1}{2}^{\circ}$ to 2° higher than the angle of the high-wing model. Therefore, the only fair comparison of the sonic-boom overpressures between the two configurations would be variation of the pressure parameter with lift coefficient as shown in figure 7. This comparison shows that, with the body below the wing, lower values of the pressure parameter are obtained throughout the positive lift range. These results indicate that no improvements in sonic-boom overpressure have been made by attempting to use the wing surface of the low-wing model as a shield to prevent the body pressures from being transmitted below the configuration toward the ground level.

CONCLUDING REMARKS

An experimental and theoretical study of the sonic-boom overpressures produced by a delta-wing-body configuration have been conducted at Mach numbers of 1.41 and 2.01. Results of the investigation indicate the following conclusions:

1. Tests of the delta-wing-body combination with the body above and below the wing showed that the measured adjusted maximum pressure-rise values were larger for the low-wing model throughout the positive lift range tested. These results indicate that the wing did not provide any beneficial shielding effect on the sonic-boom overpressures for the model with the body above the wing in the region where a finite positive lift coefficient would be required for sustained flight.

2. Comparison of the experimental and theoretical results showed good agreement which indicates that the large lift interference effects produced by the wedge-shaped body can be evaluated theoretically to obtain reasonable estimates of the sonic-boom overpressures.

Langley Research Center,
National Aeronautics and Space Administration,
Langley Station, Hampton, Va., February 25, 1966.

REFERENCES

1. Carlson, Harry W.: Correlation of Sonic-Boom Theory With Wind-Tunnel and Flight Measurements. NASA TR R-213, 1964.
2. McLean, F. Edward: Some Nonasymptotic Effects on the Sonic Boom of Large Airplanes. NASA TN D-2877, 1965.
3. Carlson, Harry W.; Mack, Robert J.; and Morris, Odell A.: Wind-Tunnel Investigation of the Effect of Body Shape on Sonic-Boom Pressure Distributions. NASA TN D-3106, 1965.
4. Mechtly, E. A.: The International System of Units – Physical Constants and Conversion Factors. NASA SP-7012, 1964.

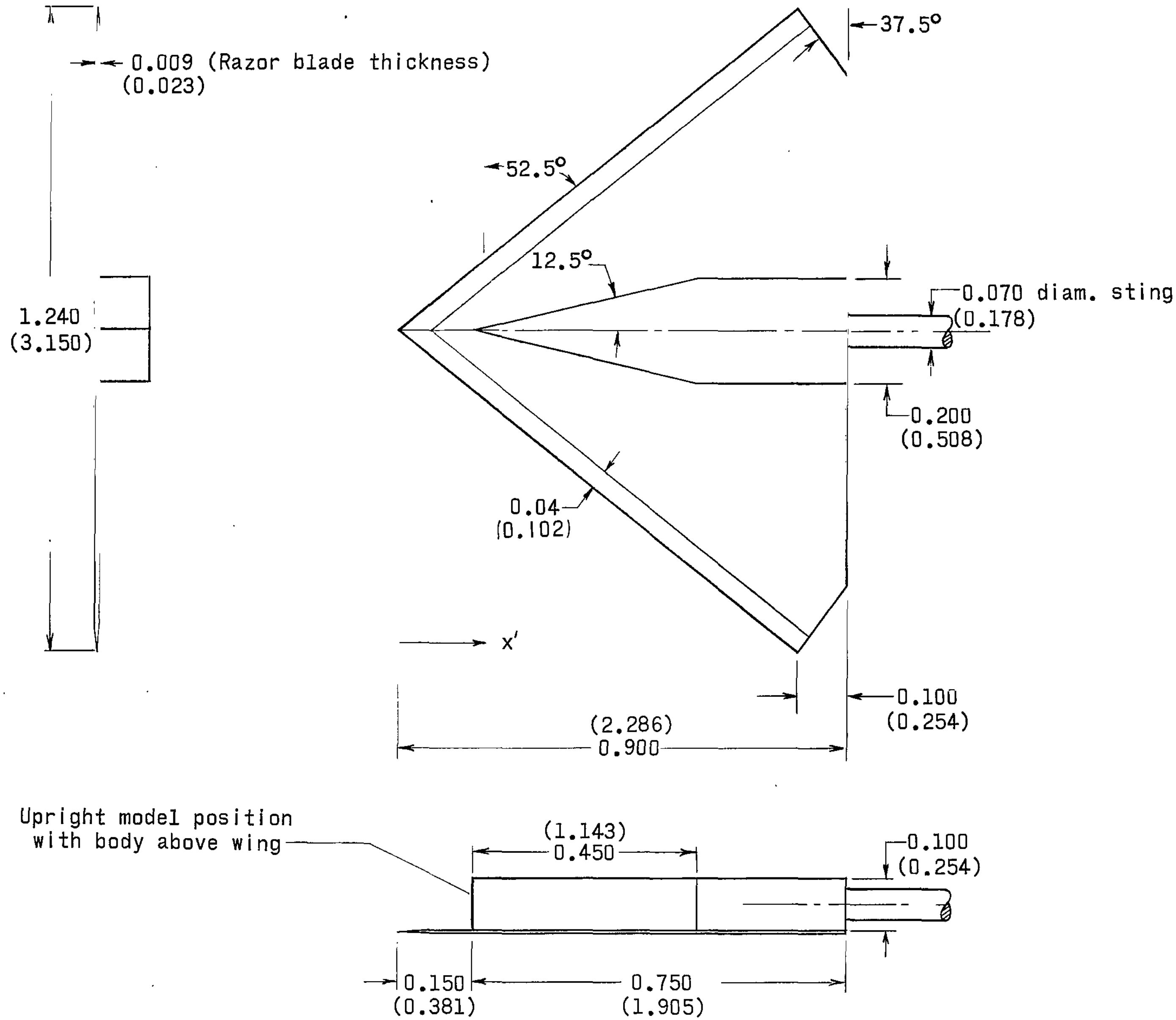

Figure 1.- Details of models.

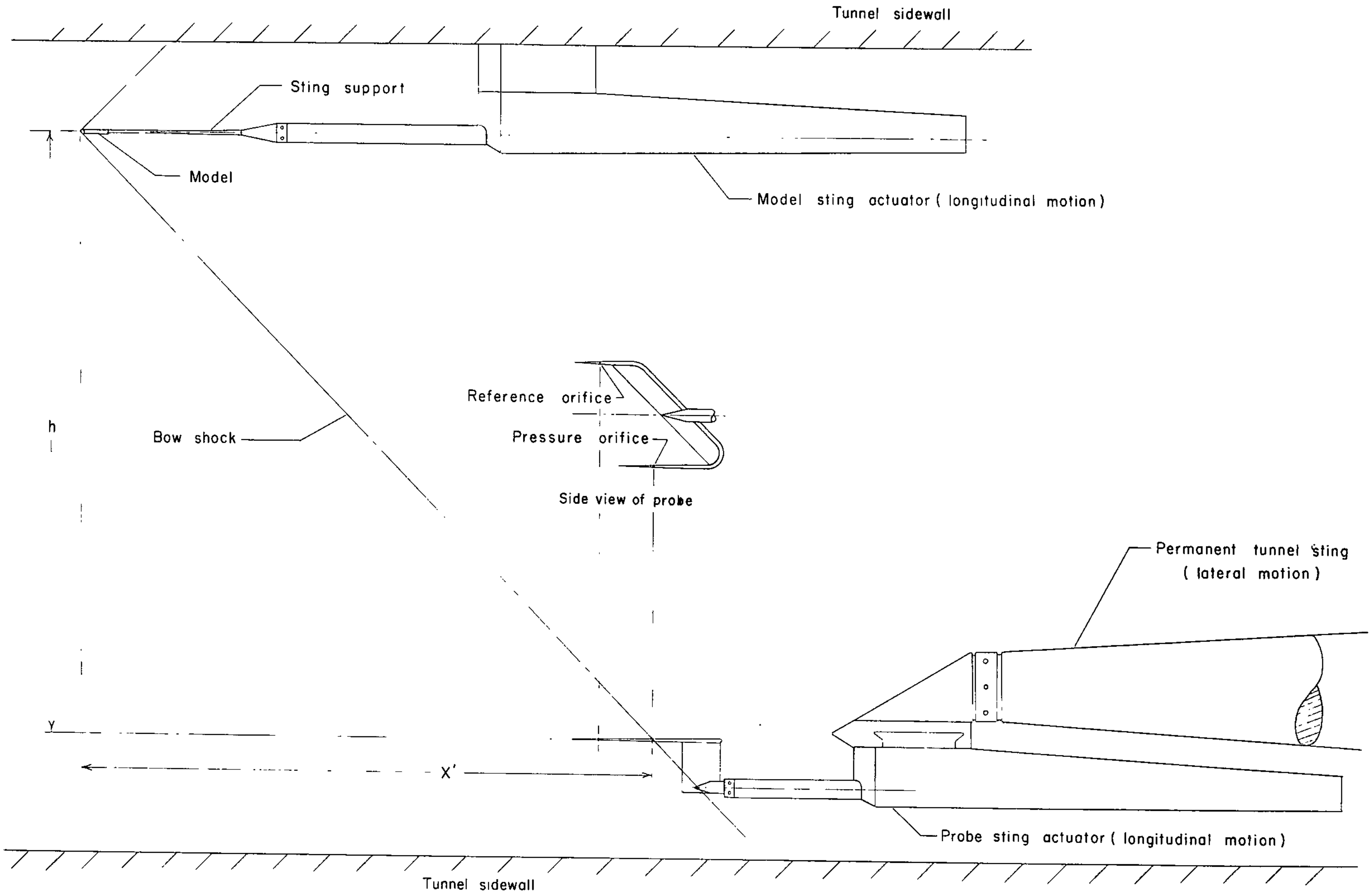

Figure 2.- Wind-tunnel apparatus.

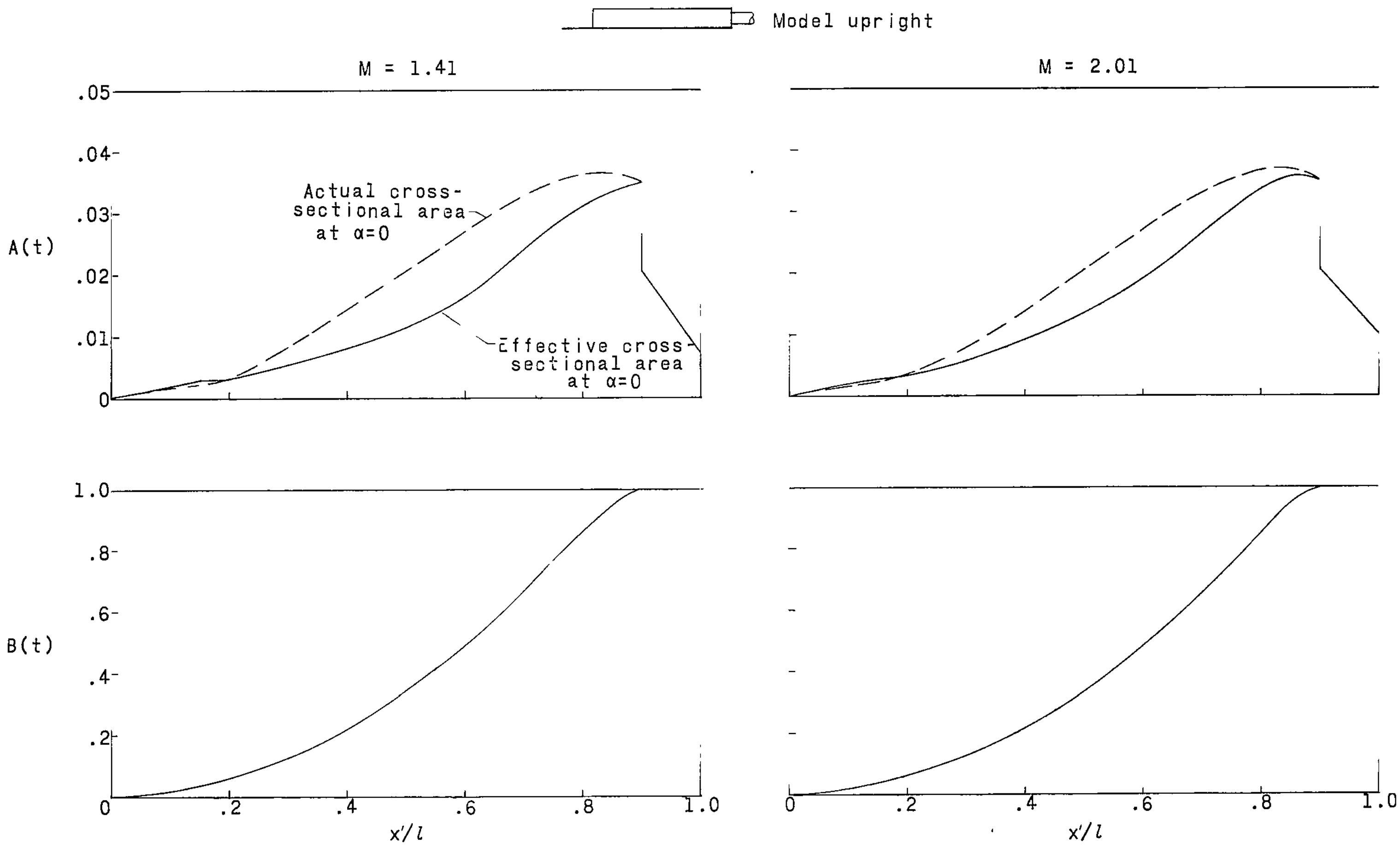

(a) Model upright.

Figure 3.- Model nondimensional cross-sectional-area distribution.

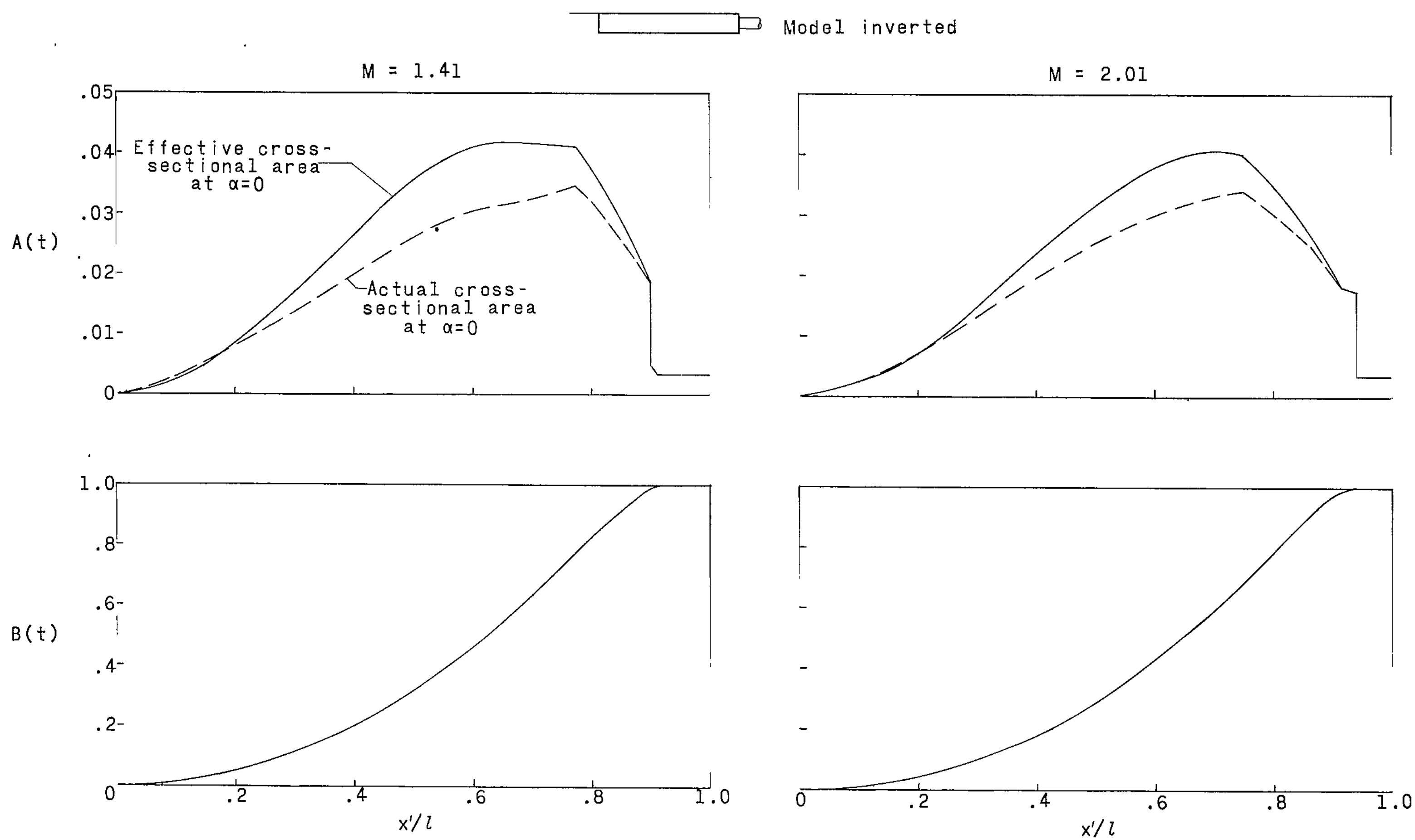

(b) Model inverted.

Figure 3.- Concluded.

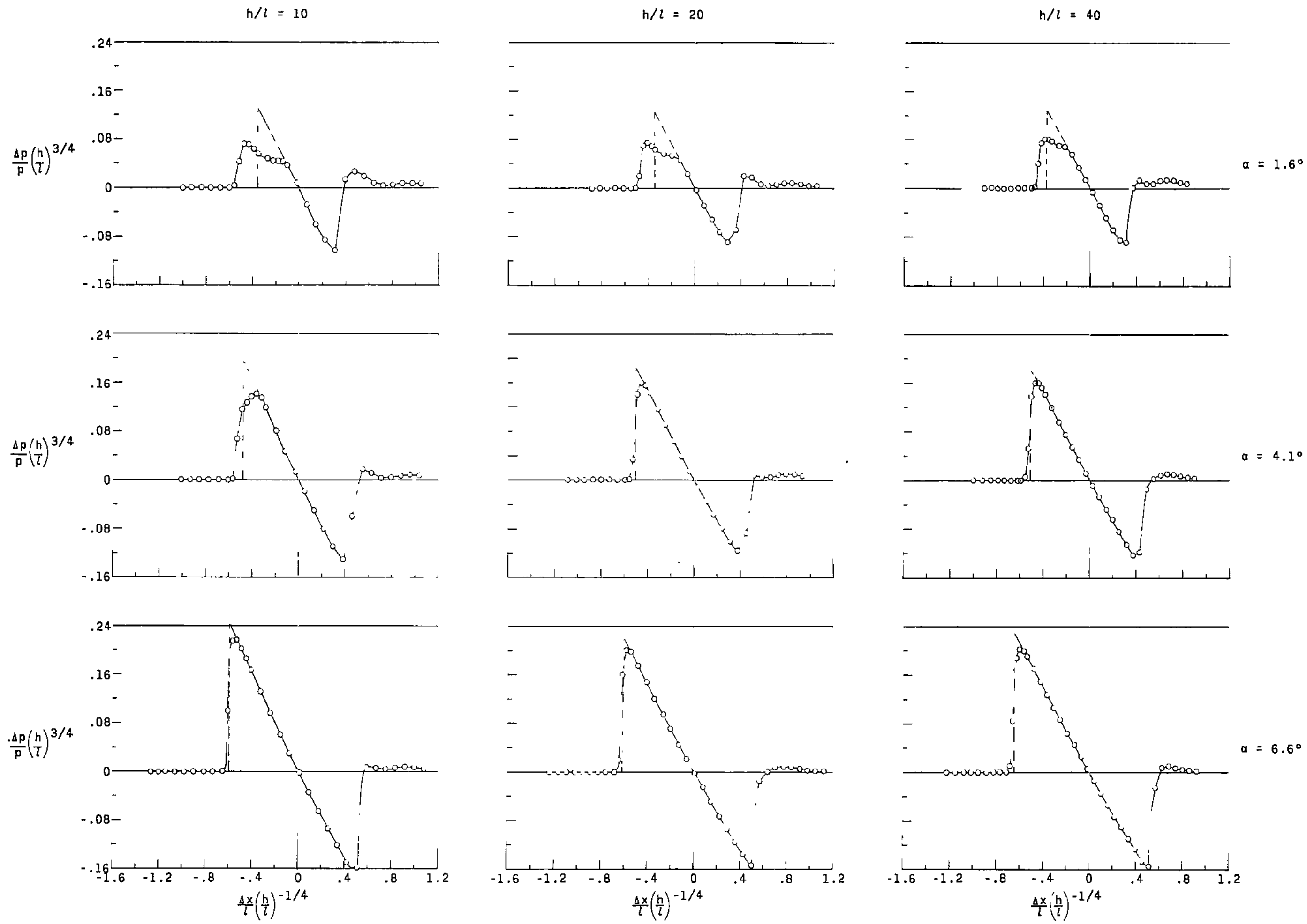

(a) Model upright, M = 1.41.

Figure 4.- Wind-tunnel measured pressure signatures. Dashed line indicates adjusted signature.

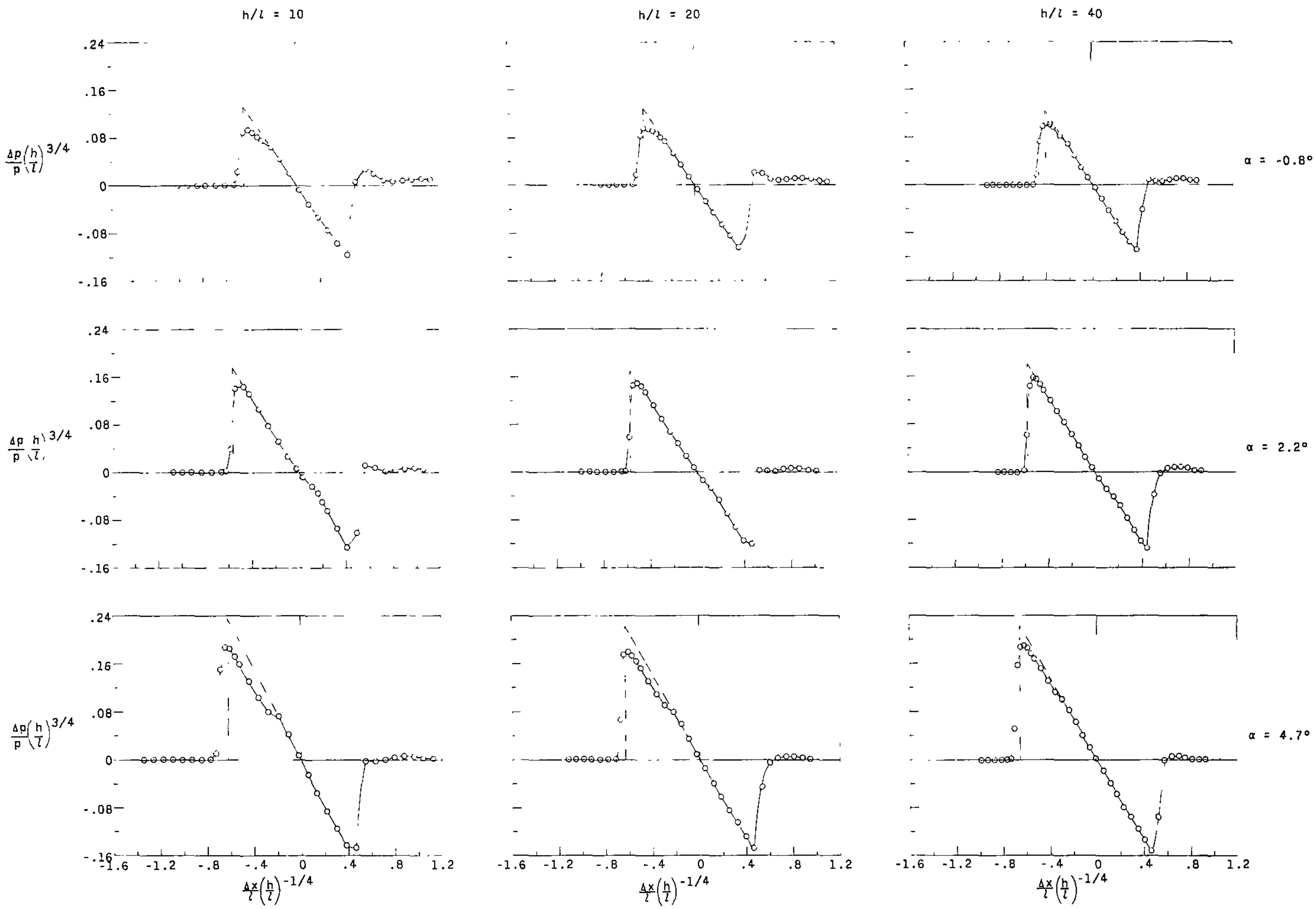

(b) Model inverted, $M = 1.41$.

Figure 4.- Continued.

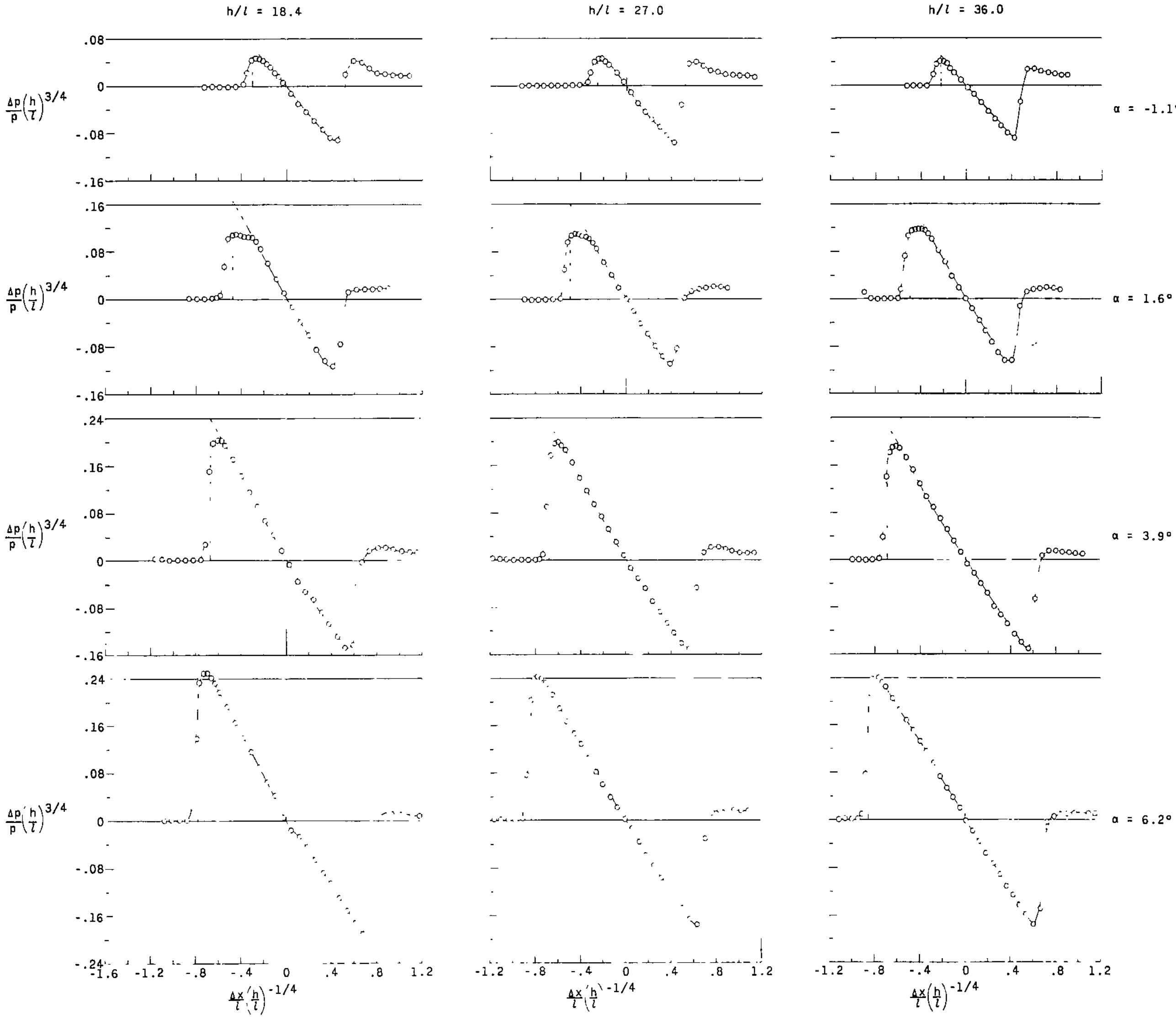

(c) Model upright, M = 2.01.

Figure 4.- Continued.

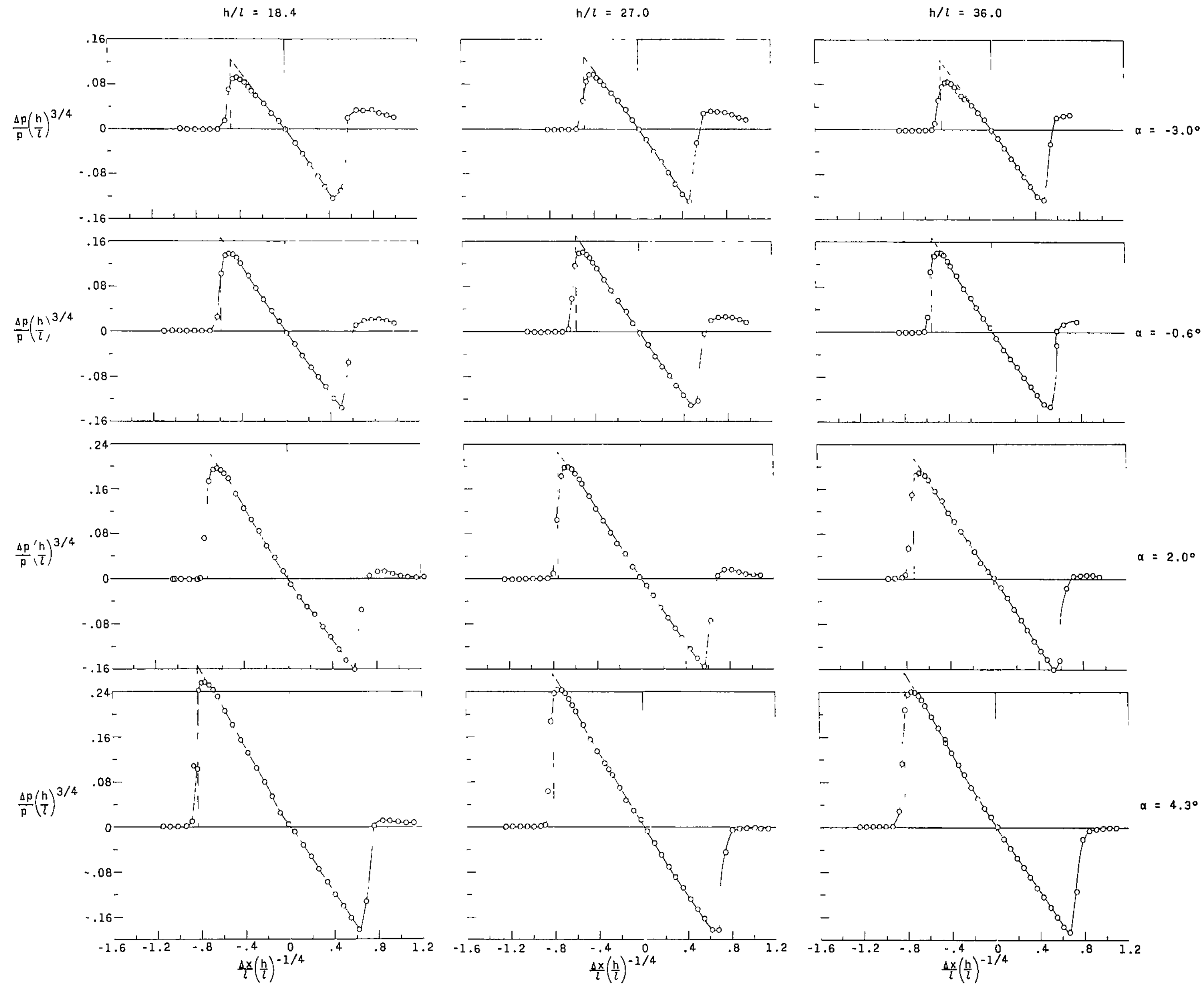

(d) Model inverted, M = 2.01.

Figure 4.- Concluded.

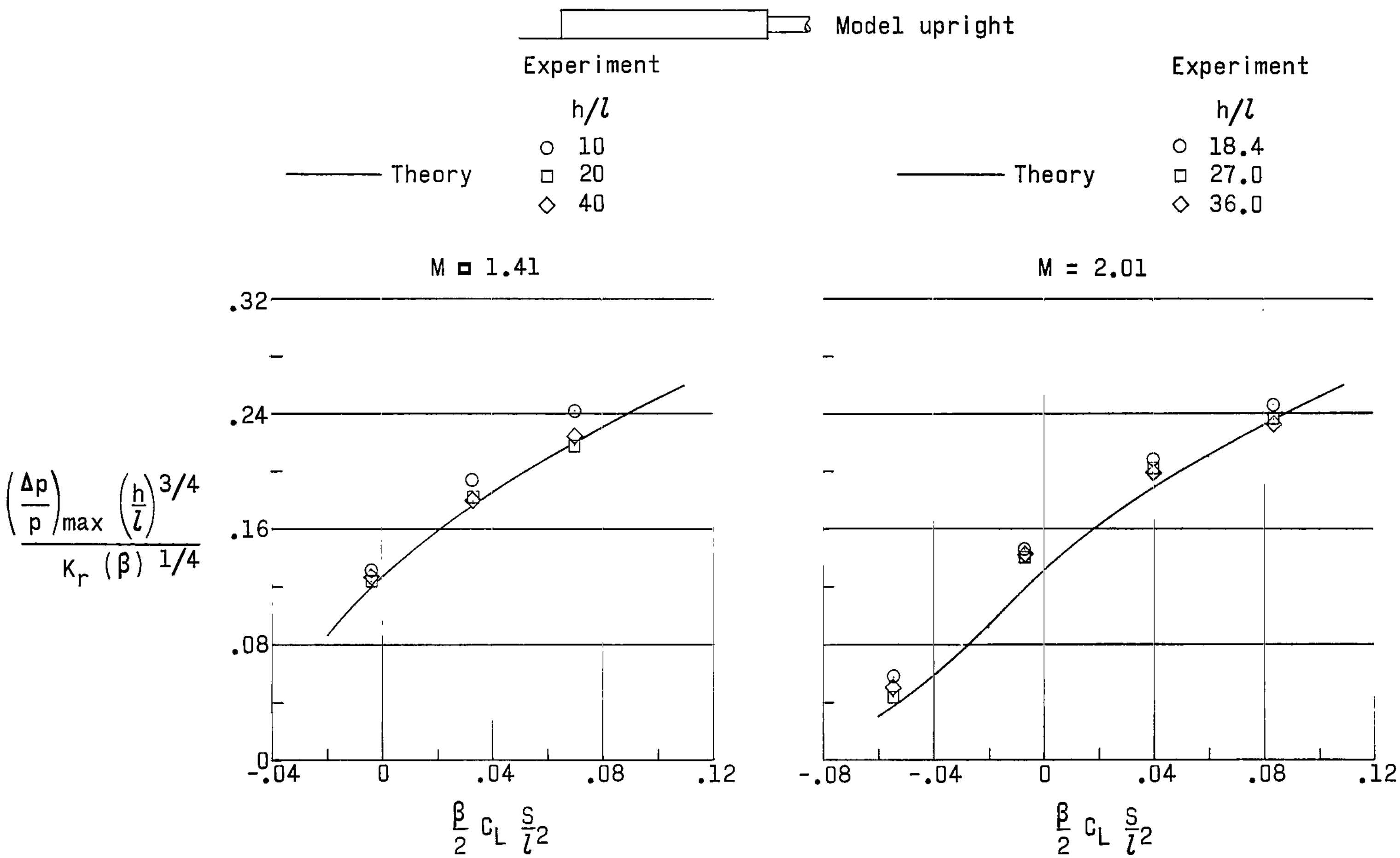

(a) Model upright.

Figure 5.- Bow-shock pressure-rise parameter for wing-body combination.

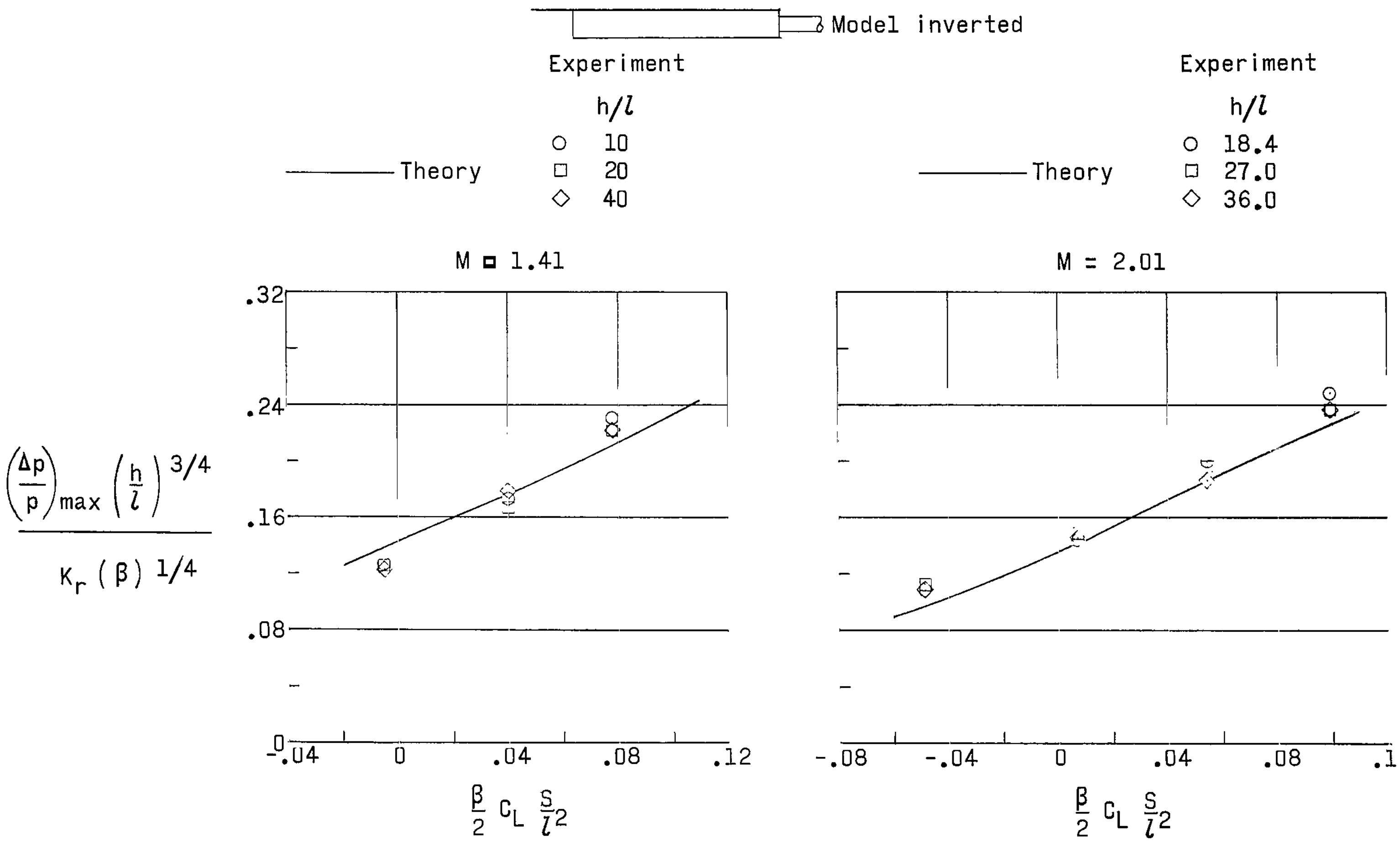

(b) Model inverted.

Figure 5.- Concluded.

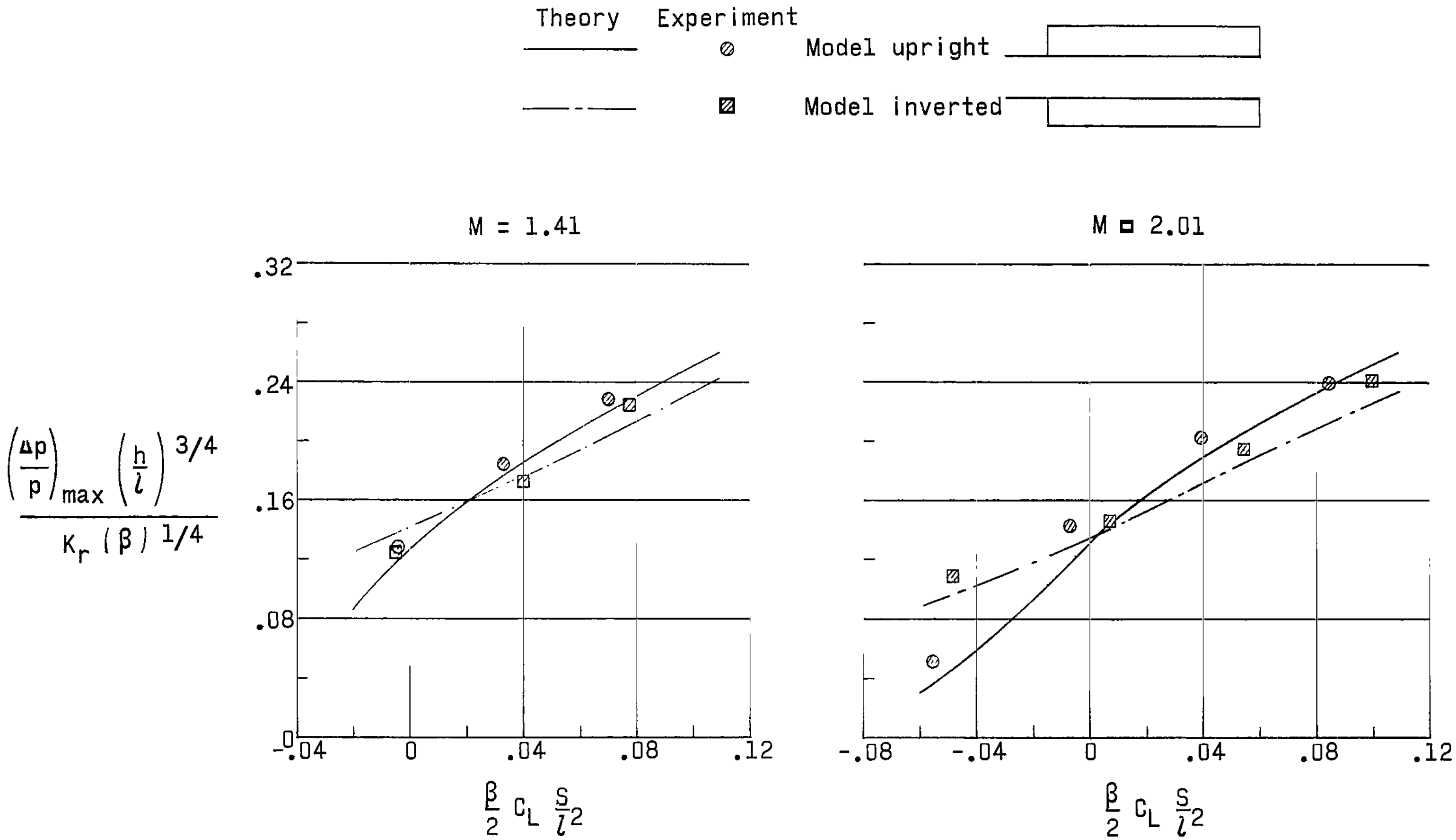

Figure 6.- Comparison of bow-shock pressure-rise parameter for model in upright and inverted positions.

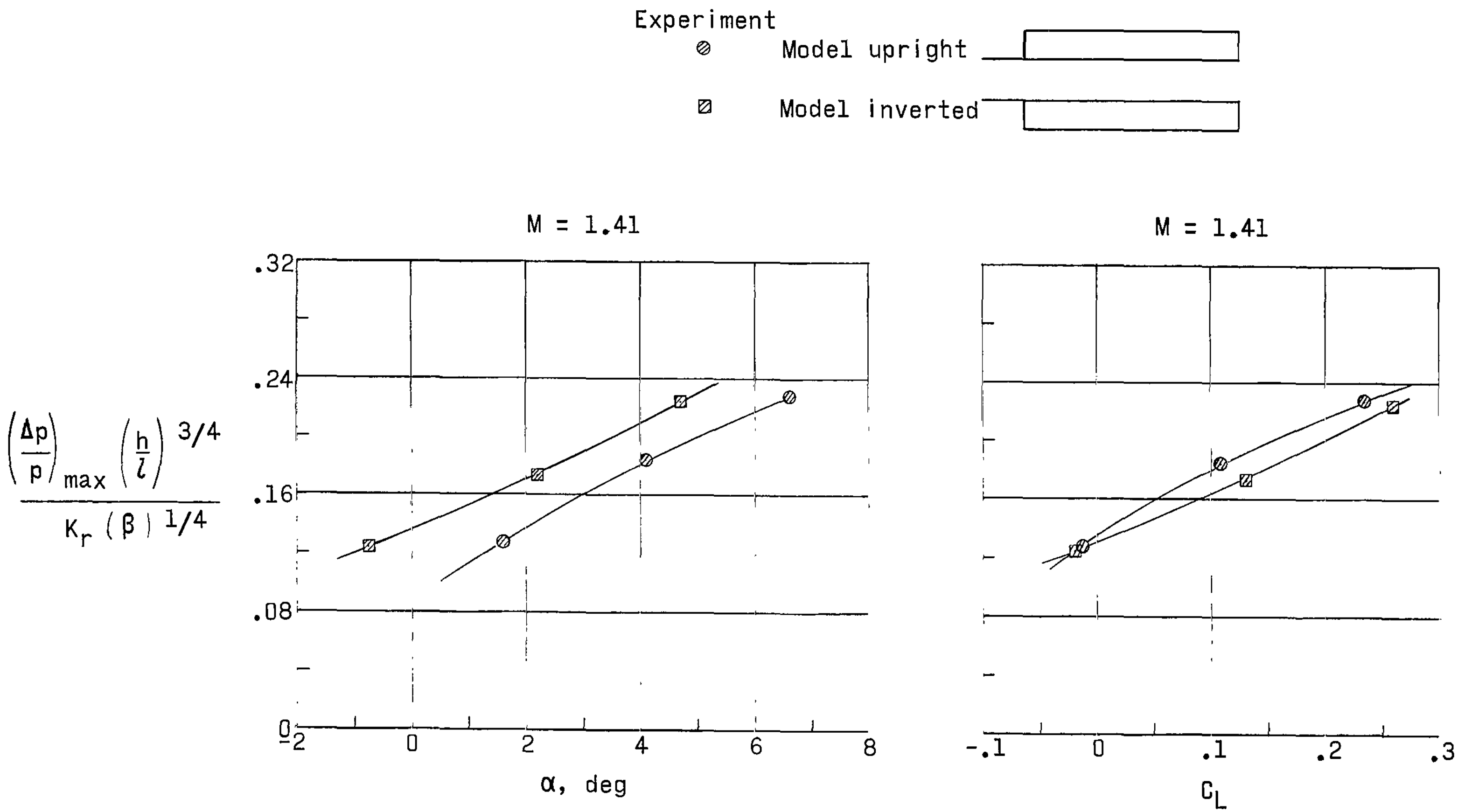

(a) M = 1.41.

Figure 7.- Variation of bow-shock pressure-rise parameter with angle of attack and lift coefficient.

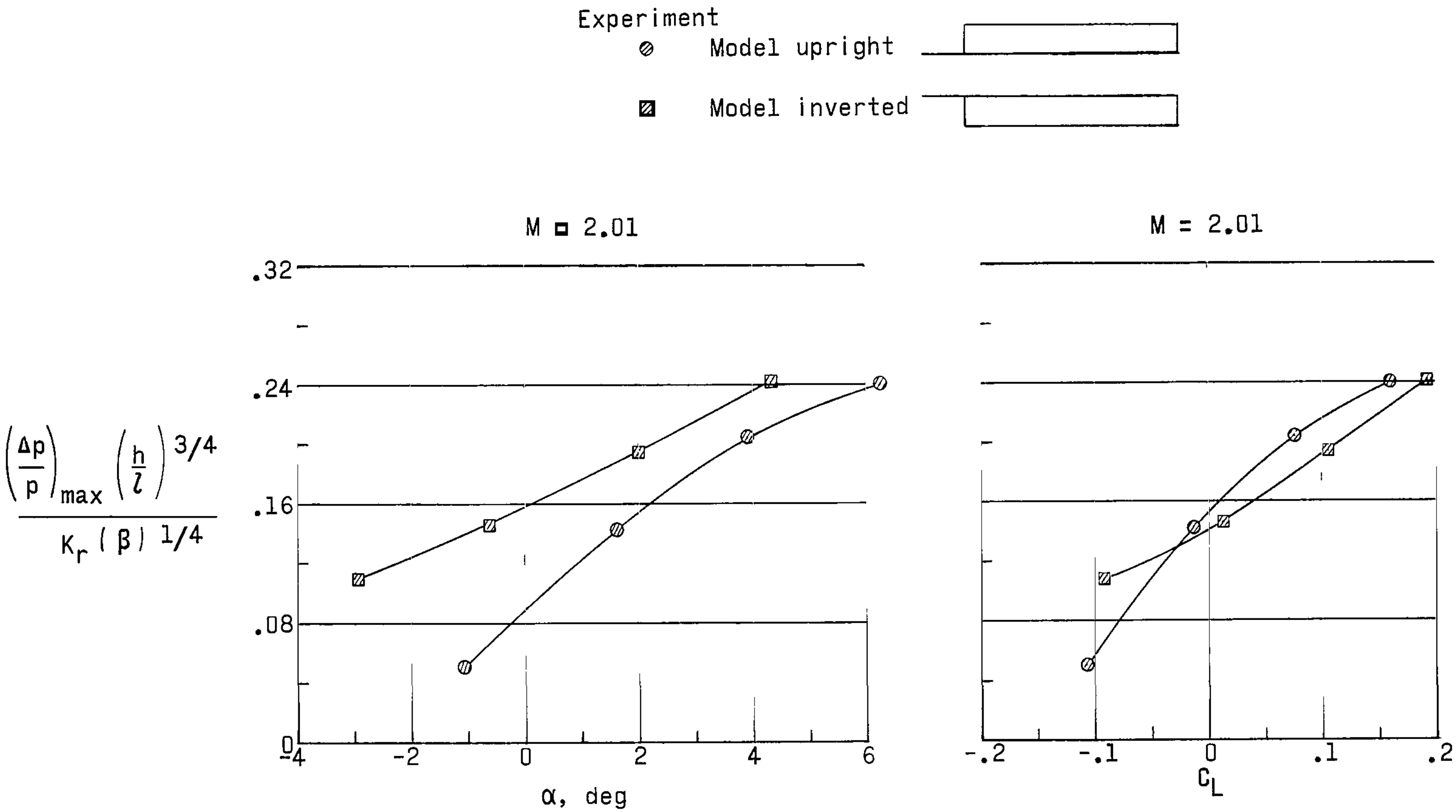

(b) M = 2.01.

Figure 7.- Concluded.

NASA-Langley, 1966 L-4882

"The aeronautical and space activities of the United States shall be conducted so as to contribute . . . to the expansion of human knowledge of phenomena in the atmosphere and space. The Administration shall provide for the widest practicable and appropriate dissemination of information concerning its activities and the results thereof."

—NATIONAL AERONAUTICS AND SPACE ACT OF 1958

NASA SCIENTIFIC AND TECHNICAL PUBLICATIONS

TECHNICAL REPORTS: Scientific and technical information considered important, complete, and a lasting contribution to existing knowledge.

TECHNICAL NOTES: Information less broad in scope but nevertheless of importance as a contribution to existing knowledge.

TECHNICAL MEMORANDUMS: Information receiving limited distribution because of preliminary data, security classification, or other reasons.

CONTRACTOR REPORTS: Technical information generated in connection with a NASA contract or grant and released under NASA auspices.

TECHNICAL TRANSLATIONS: Information published in a foreign language considered to merit NASA distribution in English.

TECHNICAL REPRINTS: Information derived from NASA activities and initially published in the form of journal articles.

SPECIAL PUBLICATIONS: Information derived from or of value to NASA activities but not necessarily reporting the results of individual NASA-programmed scientific efforts. Publications include conference proceedings, monographs, data compilations, handbooks, sourcebooks, and special bibliographies.

Details on the availability of these publications may be obtained from:

SCIENTIFIC AND TECHNICAL INFORMATION DIVISION

NATIONAL AERONAUTICS AND SPACE ADMINISTRATION

Washington, D.C. 20546